Manipulating photon emission efficiency with local electronic states in a tunneling gap

Peng Chen,[1] **Weihua Wang,**[1] **Nian Lin,**[1,2] **and Shengwang Du**[1,*]

[1]*Department of Physics, The Hong Kong University of Science and Technology, Clear Water Bay, Kowloon, Hong Kong*
[2]*phnlin@ust.hk*
[*]*dusw@ust.hk*

Abstract: We demonstrate manipulation of photon emission efficiency in a tunneling gap by tuning the rates of elastic and inelastic electron tunneling processes with local electronic states. The artificial local electronic states are created by a scanning tunneling microscope tip on a CuN nanoisland grown on a Cu(100) surface at cryogenic temperature. These local electronic states can either enhance or suppress the excitation of tip-induced surface plasmon modes at specific bias voltages, and thus the induced photon emission rates. A theoretical model quantitatively analyzing inelastic and elastic tunneling processes associated with characteristic electronic states shows good agreement with experiments. We also show that tip-induced photon emission measurement can be used for probing the electronic states in the tunneling gap.

OCIS codes: (240.6680) Surface plasmons; (240.7040) Tunneling; (300.6280) Spectroscopy, fluorescence and luminescence.

References and links

1. Y.-J. Lu, J. Kim, H.-Y. Chen, C. Wu, N. Dabidian, C. E. Sanders, C.-Y. Wang, M.-Y. Lu, B.-H. Li, X. Qiu, W. Chang, L.-J. Chen, G. Shvets, C.-K. Shih, and S. Gwo, "Plasmonic nanolaser using epitaxially grown silver film," Science **337**, 450–453 (2012).
2. K. J. Savage, M. M. Hawkeye, R. Esteban, A. G. Borisov, J. Aizpurua, and J. J. Baumberg, "Revealing the quantum regime in tunnelling plasmonics," Nature **491**, 574–577 (2012).
3. R. Esteban, A. G. Borisov, P. Nordlander, and J. Aizpurua, "Bridging quantum and classical plasmonics with a quantum-corrected model," Nat. Commun. **3**, 825 (2012).
4. N. A. Mortensen, S. Raza, M. Wubs, T. Søndergaard, and S. I. Bozhevolnyi, "Generalized nonlocal optical response in nanoplasmonics," arXiv: cond-mat/1312.7190
5. R. Berndt, J. K. Gimzewski, and P. Johansson, "Inelastic tunneling excitation of tip-induced plasmon modes on noble-metal surfaces," Phys. Rev. Lett. **67**, 3796–3799 (1991).
6. H.-M. Benia, P. Myrach, and N. Nilius, "Photon emission spectroscopy of thin MgO films with the STM: from a tip-mediated to an intrinsic emission characteristic," New J. Phys. **10**, 013010 (2008).
7. M. Reinhardt, G. Schull, P. Ebert, and R. Berndt, "Atomic resolution in tunneling induced light emission from GaAs(100)," Appl. Phys. Lett. **96**, 152107 (2010).
8. X. H. Qiu, G. V. Nazin, and W. Ho, "Vibrationally resolved fluorescence excited with submolecular precision," Science **299**, 542–546 (2003).
9. Z.-C. Dong, X.-L. Guo, A. S. Trifonov, P. S. Dorozhkin, K. Miki, K. Kimura, S. Yokoyama, and S. Mashiko, "Vibrationally resolved fluorescence from organic molecules near metal surfaces in a scanning tunneling microscope," Phys. Rev. Lett. **92**, 086801 (2004).
10. N. Nilius, N. Ernst, and H.-J. Freund, "Photon emission spectroscopy of individual oxide-supported silver clusters in a scanning tunneling microscope," Phys. Rev. Lett. **84**, 3994–3997 (2000).

#203987 - $15.00 USD Received 3 Jan 2014; revised 12 Mar 2014; accepted 14 Mar 2014; published 2 Apr 2014

11. G. Hoffmann, J. Kliewer, and R. Berndt, "Luminescence from metallic quantum wells in a scanning tunneling microscope," Phys. Rev. Lett. **87**, 176803 (2001).
12. J. K. Gimzewski, J. K. Sass, R. R. Schlitter, and J. Schott, "Enhanced photon emission in scanning tunnelling microscopy," Europhys. Lett. **8**, 435–440 (1989).
13. S. Ushioda, "Scanning tunneling microscope (STM) light emission spectroscopy of surface nanostructures," J. Electron. Spectrosc. Rel. Phenom **109**, 169–181 (2000).
14. G. Schull, N. Neel, P. Johansson, and R. Berndt, "Electron-plasmon and electron-electron interactions at a single atom contact," Phys. Rev. Lett. **102**, 057401 (2009).
15. Y. Zhang, X. Tao, H. Y. Gao, Z. C. Dong, J. G. Hou, and T. Okamoto, "Modulation of local plasmon mediated emission through molecular manipulation," Phys. Rev. B **79**, 075406 (2009).
16. F. Rossel, M. Pivetta, and W.-D. Schneider, "Luminescence experiments on supported molecules with the scanning tunneling microscope," Surf. Sci. Rep. **65**, 129–144 (2010).
17. F. Geng, Y. Zhang, Y. Yu, Y. Kuang, Y. Liao, Z. C. Dong, and J. G. Hou, "Modulation of nanocavity plasmonic emission by local molecular states of C60 on Au(111)," Opt. Express **20**, 26725–26735 (2012).
18. J. Lambe and S. L. McCarthy, "Light emission from inelastic electron tunneling," Phys. Rev. Lett. **37**, 923–925 (1976).
19. B. N. J. Persson and A. Baratoff, "Theory of photon emission in electron tunneling to metallic particles," Phys. Rev. Lett. **68**, 3224–3227 (1992).
20. P. Johansson, R. Monreal, and P. Apell, "Theory for light emission from a scanning tunneling microscope," Phys. Rev. B **42**, 9210–9213 (1990).
21. R. Berndt and J. K. Gimzewski, "Photon emission in scanning tunneling microscopy: interpretation of photon maps of metallic systems," Phys. Rev. B **48**, 4746–4754. (1993).
22. K. Perronet, L. Barbier, and F. Charra, "Influence of the Au(111) reconstruction on the light emission induced by a scanning tunneling microscope," Phys. Rev. B **70**, 201405 (2004).
23. G. Hoffmann, T. Maroutian, and R. Berndt, "Color view of atomic highs and lows in tunneling induced light emission," Phys. Rev. Lett. **93**, 076102 (2004).
24. C. Chen, C. A. Bobisch, and W. Ho, "Visualization of Fermi's golden rule through imaging of light emission from atomic silver chains," Science **325**, 981–985 (2009).
25. M. Sakurai, C. Thirstrup, and M. Aono, "New aspects of light emission from STM," Appl. Phys. A **80**, 1153–1160 (2005).
26. G. V. Nazin, X. H. Qiu, and W. Ho, "Atomic engineering of photon emission with a scanning tunneling microscope," Phys. Rev. Lett. **90**, 216110 (2003).
27. G. Schull, M. Becker, and R. Berndt,"Imaging confined electrons with plasmonic light," Phys. Rev. Lett. **101**, 136801 (2008).
28. T. Lutz, C. Große, C. Dette, C. A. Kabakchiev, F. Schramm, M. Ruben, R. Gutzler, K. Kuhnke, U. Schlickum, and K. Kern, "Molecular orbital gates for plasmon excitation," Nano Lett. **13**, 2846–2850 (2013).
29. N. L. Schneider, P. Johansson, and R. Berndt, "Hot electron cascades in the scanning tunneling microscope," Phys. Rev. B **87**, 045409 (2013).
30. F. M. Leibsle, S. S. Dhesi, S. D. Barrett, and A. W. Robinson, "STM observations of Cu(100)-c(2×2)N surfaces: evidence for attractive interactions and an incommensurate c(2×2) structure," Surf. Sci. **317**, 309–320 (1994).
31. C. D. Ruggiero, T. Choi, and J. A. Gupta, "Tunneling spectroscopy of ultrathin insulating films: CuN on Cu(100)," Appl. Phys. Lett. **91**, 253106 (2007).
32. C. F. Hirjibehedin, C.-Y. Lin, A. F. Otte, M. Ternes, C. P. Lutz, B. A. Jones, and A. J. Heinrich, "Large magnetic anisotropy of a single atomic spin embedded in a surface molecular network," Science **317**, 1199–1203 (2007).
33. S. Wang, W. Wang, Y. Hong, B. Z. Tang, and N. Lin, "Vibronic state assisted resonant transport in molecules strongly anchored at an electrode," Phys. Rev. B **83**, 115431 (2011).
34. K. Meguro, K. Sakamoto, R. Arafune, M. Satoh, and S. Ushioda, "Origin of multiple peaks in the light emission spectra of a Au(111) surface induced by the scanning tunneling microscope," Phys. Rev. B **65**, 165405 (2002).
35. P. Johansson, "Light emission from a scanning tunneling microscope: fully retarded calculation," Phys. Rev. B **58**, 10823–10834 (1998).
36. J. Aizpurua, S. P. Apell, and R. Berndt, "Role of tip shape in light emission from the scanning tunneling microscope," Phys. Rev. B **62**, 2065–2073 (2000).
37. X. Tao, Z. C. Dong, J. L. Yang, Y. Luo, J. G. Hou, and J. Aizpurua, "Influence of a dielectric layer on photon emission induced by a scanning tunneling microscope," J. Chem. Phys **130**, 084706 (2009).
38. N. Nilius, N, Ernst, and H.-J. Freund, "Tip influence on plasmon excitations in single gold particles in an STM," Phys. Rev. B **65**, 115421 (2002).
39. Z. Q. Zou, Z. C. Dong, A. K. Kar, and H. Nejo, "STM-induced photon emission spectra from the Cu(100) surface," Surf. Sci. **512**, L373–L378 (2002).
40. L. Douillard and F. Charra, "High-resolution mapping of plasmonic modes: photoemission and scanning tunnelling luminescence microscopies," J. Phys. D Appl. Phys. **44**, 464002 (2011).
41. S.-W. Hla, K.-F. Braun, V. Iancu, and A. Deshpande, "Single-atom extraction by scanning tunneling microscope tip crash and nanoscale surface engineering," Nano Lett. **4**, 1997–2001 (2004).

#203987 - $15.00 USD Received 3 Jan 2014; revised 12 Mar 2014; accepted 14 Mar 2014; published 2 Apr 2014

42. S.-W. Hla, "Scanning tunneling microscopy single atom/molecule manipulation and its application to nanoscience and technology," J. Vac. Sci. Technol. B **23**, 1351–1360 (2005).

1. Introduction

Plasmon coupled nanostructures have opened the door for emerging nanophotonics. As the gap between the metal nanostructures is reduced down to the subnanometer scale, coherent quantum tunneling of electrons dominates the plasmon modes and establishes a quantum limit for plasmonic confinement [1–4]. With the highly localized tunneling electrons, scanning tunneling microscopy (STM) is a useful tool to study photon emission phenomena at the nanoscale. STM-induced luminescence from various materials has been reported, e.g., light emission from noble metals [5], insulating films [6], semiconductors [7], molecules [8, 9], clusters [10], quantum wells [11], etc. Among these, a general mechanism is the so-called tip induced plasmon (TIP), in which local plasmon modes are excited by tunneling electrons [5, 12–17]. While the dominant portion of the tunneling current arises from elastic tunneling (ET) channels, the plasmon modes and associated photon emission are mainly excited by inelastic tunneling (IET) channels [18, 19]. It has been experimentally confirmed that the TIP photon emission depends sensitively on the density of states (DOS) of the tip and/or sample [5, 19–28]. For example, G. V. Nazin et al. showed that the DOS of a Ag chain is closely correlated with the photon yield [26]. A recent work demonstrated that the highest occupied molecular orbital (HOMO) of $Ir(ppy)_3$ molecule could act as a gate to enhance the plasmon excitation [28].

In this paper, we report on a study of using artificially-created local electronic states to enhance or suppress the efficiency of TIP photon emission. This has been achieved through altering the ratio of IET to ET in the tunneling process with local electronic states. These local states are created from monoatomic thick CuN islands, defects or atomic clusters on a Cu(100) surface. We demonstrate that, under a positive bias voltage, the TIP photon emission efficiency can be enhanced or suppressed as large as two orders of magnitude by manipulating the local electronic states associated with these nanostructures. A theoretical model which accounts the local-state contribution in calculating the ET and IET tunneling rates shows good agreement with the experimental results. Moreover, we also show the ability of reconstructing of DOS with photon emission data. Our findings may lead to applications in designing and engineering nanophotonic devices at the quantum tunneling regime.

2. Theoretical model

As illustrated in Fig. 1, electrons tunnel between the tip and metal sample surface through both ET and IET channels. Photon emission occurs in the IET channels where the electrons are coupled with the surface plasmon modes under the energy conservation [13, 19]. As compared to the ET process, the portion of the IET process is often very low. When an electron tunnels from the tip to the sample (Figs. 1(a) and 1(b), $V_b > 0$), following the Fermi's golden rule [19, 24, 29], we can obtain the rates of ET and IET processes

$$w_e(V_b) = \frac{2\pi}{\hbar}\int_{E_F}^{E_F+eV_b}\rho_t(\varepsilon)\rho_s(\varepsilon)|M_e|^2 d\varepsilon, \quad (1)$$

$$w_{in}(V_b) = \frac{2\pi}{\hbar}\int_{E_F}^{E_F+eV_b-h\nu}\rho_t(\varepsilon+h\nu)\rho_s(\varepsilon)|M_{in}|^2 d\varepsilon, \quad (2)$$

where E_F is the Fermi energy level of the sample. V_b is the bias voltage between the sample and the tip, $\rho_t(\varepsilon)$ and $\rho_s(\varepsilon)$ are the DOS of the tip and the sample, respectively. M_e and M_{in} are the

#203987 - $15.00 USD Received 3 Jan 2014; revised 12 Mar 2014; accepted 14 Mar 2014; published 2 Apr 2014

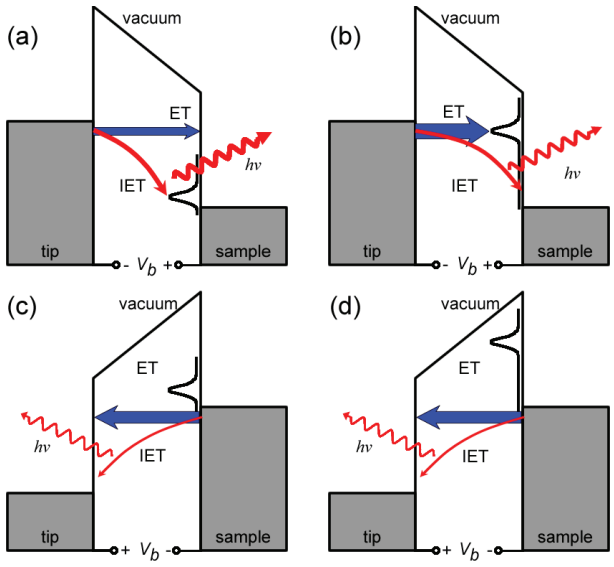

Fig. 1. Electrons tunnel between the STM tip and the metal sample surface with an applied bias voltage V_b. The local electronic state density is denoted by black curves. (a) $V_b > 0$: The IET process and related photon emission are enhanced due to the local states close to the sample Fermi level. (b) $V_b > 0$: The ET process is enhanced due to the local states close to the Fermi level of the tip, which suppresses the inelastic tunneling process and photon emission. (c) and (d): Under a negative bias voltage ($V_b < 0$), both ET and IET channels are not affected by local states of the sample.

corresponding transition matrix elements of the ET and IET processes. $h\nu$ is the photon energy. If a local electronic state is present on the sample surface above the Fermi level, as exemplified in Figs. 1(a) and 1(b), assuming $\rho_t(\varepsilon)$, M_e, and M_{in} vary slowly with the energy ε in the interval $E_F < \varepsilon < E_F + eV_b$, Eq. (2) can be approximated as

$$w_{in}(V_b) \approx \frac{|M_{in}|^2}{|M_e|^2} w_e(V_b - h\nu/e). \tag{3}$$

We therefore obtain the probability for an electron to tunnel inelastically, which accounts for plasmon excitation and the induced photon emission, as

$$P(V_b) = \frac{w_{in}}{w_e + w_{in}} \approx \frac{w_{in}}{w_e} \approx \frac{|M_{in}|^2}{|M_e|^2} \frac{w_e(V_b - h\nu/e)}{w_e(V_b)}. \tag{4}$$

Hence the portion of inelastic tunneling electrons at a given bias voltage depends on the characteristic distribution of $\rho_s(\varepsilon)$. For the case illustrated in Fig. 1(a), where the local electronic state is close to the sample Fermi level, the IET probability is enhanced because $w_e(V_b - h\nu/e)$ occupies a large portion of $w_e(V_b)$. For the case shown in Fig. 1(b), the local electronic state close to the tip Fermi level enhances the ET process and thus suppresses the efficiency of plasmon-induced photon emission in the IET channel. In contrast, with negative bias (electrons tunnel from the sample to the tip, Figs. 1(c) and 1(d)), since the local states are all above the sample Fermi level, both $\rho_t(\varepsilon)$ and $\rho_s(\varepsilon)$ vary slowly within the interval $E_F - eV_b < \varepsilon < E_F$. In these two cases, the IET probabilities are not affected by the presence of sample local electronic states [19].

#203987 - $15.00 USD Received 3 Jan 2014; revised 12 Mar 2014; accepted 14 Mar 2014; published 2 Apr 2014

Since the plasmon-induced photon emission yield scales linearly with the amount of inelastic electrons, the photon emission rate can be expressed as $R_{h\nu} = \eta I_0 P$, where I_0 is the total tunneling current and η is a grouped constant determined by the gap geometry and photon collecting efficiency. The ratio in Eq. (4) could be obtained from photon emission spectral data and site-dependent scanning tunneling spectroscopy (STS, dI/dV_b spectra) data experimentally.

For $V_b > h\nu/e$

$$R_{h\nu}(V_b) \propto \frac{w_e(V_b - h\nu/e)}{w_e(V_b)} = \frac{\int_0^{V_b - h\nu/e} \frac{dI}{dV} dV}{\int_0^{V_b} \frac{dI}{dV} dV}. \tag{5}$$

For $V_b < 0$ and $|V_b| > h\nu/e$ when the electrons tunnel from the sample to the tip,

$$R_{h\nu}(V_b) \propto \frac{w_e(V_b + h\nu/e)}{w_e(V_b)} = \frac{\int_0^{V_b + h\nu/e} \frac{dI}{dV} dV}{\int_0^{V_b} \frac{dI}{dV} dV}. \tag{6}$$

3. Experiment

We carry out the experiments in an ultra-high vacuum (UHV) STM system (Omicron) operated at the temperature of 4.9 K. CuN nanoislands are grown on a single-crystal Cu(100) substrate following the reported method [30]. The photons are collected with a lens mounted outside the UHV chamber, and coupled into a spectrometer (SpectraPro SP2356) pre-cooled at -80 $^\circ$C through a multimode optical fiber. The typical collection efficiency is about 10^{-6} s^{-1} per tunneling electron. The photon counts are measured by the spectrometer in the focus mode, with a measurement time of 10 s.

Figure 2(a) lower inset is a typical STM topograph of the CuN/Cu(100) substrate. The dark regions are monoatomic thick CuN nanoislands which show a lower apparent height than Cu. Note the lower apparent height is not a geometrical effect, but attributed to decreased density of electronic states of CuN film [31]. We frequently find some defects with higher apparent height on CuN nanoislands, as the one marked by the white circle. Since this defect could not be moved by the STM tip, we assume that it is a missing-N defect. The side-view of the atomic structures of Cu, CuN and a missing-N defect is depicted in the upper inset of Fig. 2(a). The relative positions of N atoms with respect to Cu atoms are plotted according to ref. [32]. The differential conductance spectra, which reflect the local DOS, measured over Cu, CuN and the defect are shown in Fig. 2(a). The spectrum of Cu shows a broad and weak peak around 1.6 V, which is associated with an unoccupied surface resonance [31]. The spectrum of CuN shows very weak signal in the bias range of -3 V to 1.5 V, a steep increase above 2.0 V, and a strong peak at 2.3 V [31, 33]. The spectrum of the defect shows similar feature as CuN below 2 V, and exhibits a shoulder at about 2.2 V.

Figures 2(c) and 2(d) display photon emission spectra acquired at Cu, CuN and the defect. We notice that the spectral line shapes of TIP photon emission are sensitive to the tip geometry [34–38]. In this work, to confirm clearly the electronic state effects and rule out others, we carefully avoid changing the tip while conducting a complete set of measurements. The spectra are monitored before and after the measurement of photon emission rate. If the tip is found changed, the measurement of photo emission rate will be repeated. The tip-sample separation

#203987 - $15.00 USD Received 3 Jan 2014; revised 12 Mar 2014; accepted 14 Mar 2014; published 2 Apr 2014

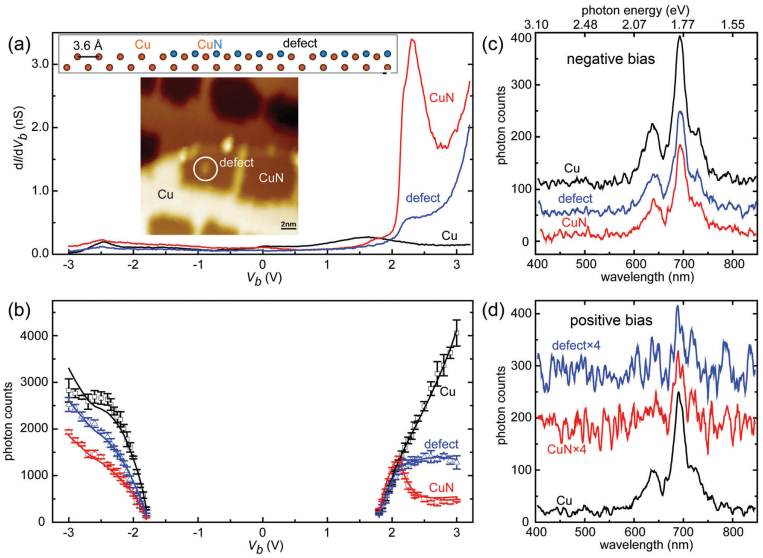

Fig. 2. (a) Site-dependent scanning tunneling spectroscopy (STS, dI/dV_b spectra) measured over Cu, CuN and defect. Lower inset: STM topograph of CuN nanoislands on a Cu(100) surface, with a defect marked by the white circle (16×16 nm^2, 1.0 V and 0.5 nA). Upper inset: Side view of the atomic structure of Cu, CuN and a missing-N defect. (b) Photon counts as functions of bias voltages V_b. The experimental data are measured over 5 times, drawn by symbols with error bars. The solid curves are calculated from the dI/dV_b spectra following Eqs. (5) and (6). (c) and (d): Photon spectra measured at Cu, CuN and defect in the case of negative bias or positive bias voltages ($\mp$3.0 V, 20 nA, 450 s). The spectra are shifted vertically for clarity.

is about 0.5 nm at the tunneling regime with STM. The usual curvature radius of the tip is dozens of nm. In this case, variation of spectral line shapes with different bias voltages is unremarkable. [5,20,37,39,40]. As revealed in Figs. 2(c) and 2(d), the line shapes of six photon spectra are nearly identical with a central wavelength of 700 nm ($h\nu = 1.77$ eV). Therefore the photon emission acquired at CuN and the defect is of the same plasmon modes as that of Cu. This photon energy coincides with the threshold electron energy of 1.77 eV for all the six cases, indicating the photon emission arises from a radiative decay of the localized surface plasmon induced in the tunneling gap by the IET electrons [5, 16].

Figure 2(b) shows the photon counts as functions of bias voltages measured at Cu, CuN and the defect in the constant tunneling current mode. At negative bias voltages, the photon counts measured at three structures all increase monotonously with the bias voltage, consistent with the prediction of Eq. (2) in Ref. [19]. At positive bias voltages, the photon counts acquired at Cu surface also show monotonously rising trend with the increase of bias voltage. In contrast, the photon counts acquired with the tip located on CuN nanoisland display a resonance-like peak at $V_b = 2.1$ V, while the photon counts measured at the defect show a saturation behavior for $V_b > 2.1$ V. At $V_b = 3$ V, the photon rate is suppressed by a factor of 8 at CuN compared to the bare Cu. Based on the dI/dV_b data shown in Fig. 2(a), we simulate the photon counts as a function of bias voltage following Eqs. (5) and (6). In the simulation, we set $h\nu = 1.77$ eV and numerically sum the STS data to calculate the integrations. The only fitting parameter is a prefactor ($\eta|M_{in}|^2/|M_e|^2$) that accounts for the transmission matrix elements of the ET and IET processes and the photon collecting efficiency. The results are shown as the solid curves

#203987 - $15.00 USD Received 3 Jan 2014; revised 12 Mar 2014; accepted 14 Mar 2014; published 2 Apr 2014

in Fig. 2(b), which fit the measured photon emission data very well for all three structures at both positive and negative bias voltages. The good agreement between the simulated and the experimental photon counts indicates that our simple model can quantitatively describe the TIP photon emission rate. The suppression of the TIP photon emission at CuN for $V_b > 2.1$ V is associated with the emergence of the local electronic states of CuN above 2.0 V, which effectively enhances (suppresses) the ET (IET) process as illustrated in Fig. 1(b). Similarly the local states of the defect enhance the ET process too, but the local states are not as strong as those of CuN, so the photon counts saturate at $V_b > 2.1$ V instead of decaying. In the case of negative bias, the photon counts of the three structures do not exhibit significant difference, which can be understood by the process illustrated in Fig. 1(d).

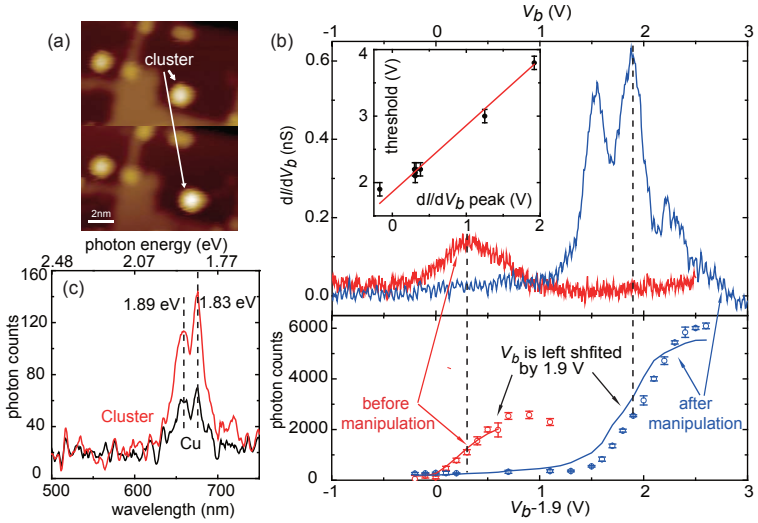

Fig. 3. Manipulating photon emission efficiency with local electronic states from an artificial cluster. (a) STM topographs of a cluster (marked by the arrow) before (upper panel) and after (lower panel) manipulation (12×8 nm^2, 1.0 V and 0.5 nA). (b) dI/dV_b spectra (upper panel) and photon counts (lower panel) with different bias voltages measured at the arrow-marked cluster before and after manipulation. In the lower panel, the experimental data are measured over 3 times, drawn by symbols with error bars; the simulation are drawn by solid curves. (c) Photon spectra measured over Cu and the cluster (3.0 V, 20 nA, 450 s).

As illustrated in Fig. 1(a) and quantitatively described in our model, we expect that creating a local electronic state close to the sample Fermi level may allow us to enhance the IET process and thus the photon emission. To demonstrate the ability of controlling and manipulating the TIP photon emission efficiency, we create some artificial atomic clusters that have distinguished local electronic states. The clusters are produced by dipping the tip into the Cu substrate [41,42]. The STM topograph in the upper panel of Fig. 3(a) shows three clusters located on CuN islands. We manipulate a cluster (marked by the arrow) by the STM tip. The lower panel of Fig. 3(a) shows that the cluster is moved to a new position. Before manipulation, The cluster has a local electronic state around 0.3 V, which is close to the sample Fermi level, as shown in the upper panel of Fig. 3(b). After manipulation, the cluster no longer shows the state at 0.3 V, but two strong new states at 1.6 V and 1.9 V. The change of electronic states of cluster may be due to variation of adsorption on CuN island. The photon emission results acquired with the tip located at the cluster before and after the manipulation are shown in the lower panel of Fig. 3(b). Before manipulation, the threshold bias voltage for photon emission is 2.2 V, which is 1.9 V higher

#203987 - $15.00 USD Received 3 Jan 2014; revised 12 Mar 2014; accepted 14 Mar 2014; published 2 Apr 2014

than the energy of the 0.3 V state. This shift of 1.9 V equals the characteristic photon energy as shown in Fig. 3(c). After manipulation, the threshold bias voltage for photon emission shifts to 3.8 V. The offset between this threshold and the cluster state after manipulation is still 1.9 V, as shown in Fig. 3(b). This result can be understood as following: assuming that a local electronic state lies at V above the sample Fermi level, the threshold bias voltage required to excite surface plasmon modes is $V + h\nu/e$. As a result, shifting the local electronic state of the cluster changes the threshold bias voltage. We simulate the photon counts of the cluster before and after the manipulation according to Eqs. (5) and (6) using the corresponding $\mathrm{d}R_{h\nu}/\mathrm{d}V_b$ data and setting $h\nu = 1.9$ eV. The simulated photon counts are plotted as solid curves in the low panel of Fig. 3(b), which fit the experimental data very well. We have made and measured six clusters totally. Their electronic states energy levels and threshold bias voltages are plotted in the inset in Fig. 3(b), where the red line displays $V_{threshold} = V_{state} + 1.9$ V. One can see that all the experimental data fall on or near the red line, confirming the proposed mechanism of using local electronic states to control the inelastic tunneling efficiency. It is worthwhile to note that the photon counts acquired at the clusters can reach 90 times of those on CuN under the same experimental conditions. To test the scenario illustrated in Fig. 1(c), we measure the photon emission on these clusters with negative bias voltage and found that the emission rate behaved similarly as the bare CuN. The clusters' local electronic states do not enhance or suppress the TIP photon emission, consistent with the prediction of our model.

4. Reconstruction of DOS

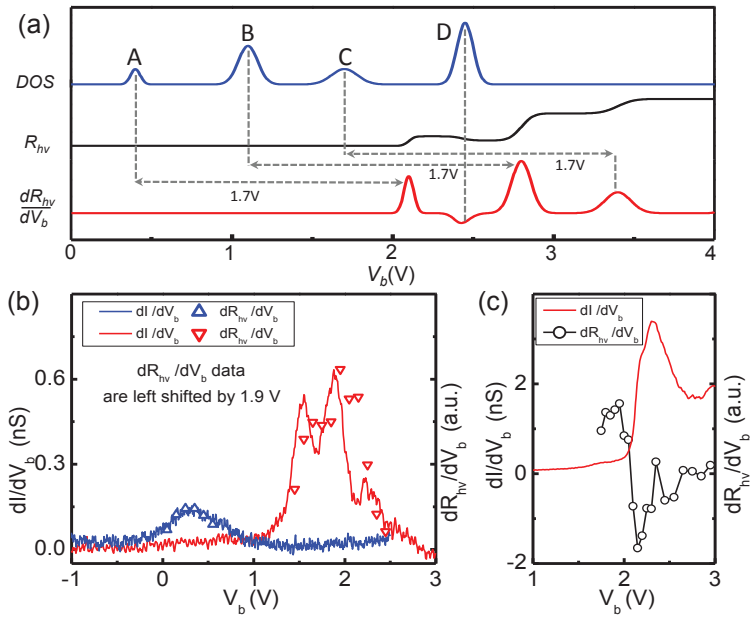

Fig. 4. Reconstructing local DOS from the photon emission data. (a) An arbitrary DOS, photon emission rate $R_{h\nu}$ and its derivative $\mathrm{d}R_{h\nu}/\mathrm{d}V_b$. (b) The calculated $\mathrm{d}R_{h\nu}/\mathrm{d}V_b$ (down-shifted by 1.9 V) from the photon emission data as compared with the STS spectra of the cluster ($\mathrm{d}R_{h\nu}/\mathrm{d}V_b$) before and after manipulation (the marked cluster in Fig. 3(a)). (c) The calculated $\mathrm{d}R_{h\nu}/\mathrm{d}V_b$ as compared with STS spectrum of CuN ($\mathrm{d}I/\mathrm{d}V_b$).

Next, we confirm that the local DOS of the sample surface can be reconstructed from the

#203987 - $15.00 USD Received 3 Jan 2014; revised 12 Mar 2014; accepted 14 Mar 2014; published 2 Apr 2014

photon emission data [26]. From Eq. (4) and $R_{h\nu} = \eta I_0 P$, we can derive

$$\frac{dR_{h\nu}}{dV_b} \approx \frac{1}{w_e(V_b)} \left[\eta I_0 \rho_s (eV_b - h\nu) - R_{h\nu}\rho_s (eV_b)\right]. \quad (7)$$

Hence, the derivative of photon emission rate with respect to bias voltage can be used to trace back the DOS characteristics of the sample under the condition that the tip possesses a slowly varying DOS distribution. As an example, we plot an arbitrary DOS distribution shown by the upper curve in Fig. 4(a). The calculated photon rate $R_{h\nu}$ with $h\nu = 1.7$ eV is drawn by the middle curve according to Eq. (4). The lower curve gives $\mathrm{d}R_{h\nu}/\mathrm{d}V_b$. From Eq. (7), the positive peaks in $\mathrm{d}R_{h\nu}/\mathrm{d}V_b$ are corresponding to IET channels at energy of $eV_b - h\nu$, while negative dips are associated with ET channels at energy of eV_b. Therefore we can assign the three positive peaks in $\mathrm{d}R_{h\nu}/\mathrm{d}V_b$ to the electronic states A, B and C, which are 1.7 eV down-shifted, and the negative dip to state D at the same energy. Figure 4(b) shows the derivative data of $\mathrm{d}R_{h\nu}/\mathrm{d}V_b$ (up and down triangles) measured at the cluster before and after manipulation (the marked cluster in Fig. 3(a)) towards the $\mathrm{d}I/\mathrm{d}V_b$ spectra, where the $\mathrm{d}R_{h\nu}/\mathrm{d}V_b$ data are downshifted by the photon energy of 1.9 eV. The $\mathrm{d}R_{h\nu}/\mathrm{d}V_b$ data nicely reconstruct the characteristic local electronic states revealed by STS spectra. Figure 4(c) shows the derivative data of $\mathrm{d}R_{h\nu}/\mathrm{d}V_b$ measured on CuN as compared with its $\mathrm{d}I/\mathrm{d}V_b$ spectrum. The negative dip in $\mathrm{d}R_{h\nu}/\mathrm{d}V_b$ is associated with the 2.3 V peak in the DOS of CuN.

5. Conclusion

In summary, we have demonstrated that the TIP photon emission efficiency can be manipulated by controlling the IET and ET processes with local electronic states in a STM tunneling gap. With artificial nanostructures, we can either open or close the IET channel and thus enhance or suppress the plasmon excitation. The theoretical model taking into account the contribution of the local DOS agrees well with the experimental data. We'd like to emphasize that in this work we do not intend to provide a new description of the origin of the STM-stimulated photon emission; instead, we have formulated a relationship between local electronic states and the efficiency of TIP photon emission. This relationship is found to be general, which is rooted in the Fermi's golden rule, and independent of the origin of the electronic states or the tip structure. Moreover, this relation allows us to manipulate the photon emission efficiency through creating artificial electronic states. These results have demonstrated that experimentally-measured TIP photon emission efficiency can be quantitatively described by a theoretical formulation which computes ET and IET tunneling processes, providing useful guidance for designing and engineering nanophotonic devices in the subnanometer scale.

Acknowledgments

The work is partially supported by HKUST under the internal Research Equipment Competition Fund and the Hong Kong Research Grants Council (Project Nos. HKU8/CRF/11G and HKUST2/CRF/10). The authors acknowledge S. Wang and T. Lin for technical assistance, and S. Zhang for helpful discussion. Peng Chen and Weihua Wang contribute equally to this work.

#203987 - $15.00 USD Received 3 Jan 2014; revised 12 Mar 2014; accepted 14 Mar 2014; published 2 Apr 2014